Direct Comparison of Electron Transfer Properties of Two Distinct Semisynthetic Triads with Non-Protein Based Triad: Unambiguous Experimental Evidences on Protein Matrix Effects

Yi-Zhen Hu,[a] Hiroshi Takashima,[a] Shinya Tsukiji,[a] Seiji Shinkai,[a] Teruyuki Nagamune,[b] Shigero Oishi,[c] and Itaru Hamachi*[a]

Abstract: In order to understand the roles of protein matrix in electron transfer processes (ET) within biological systems, a heme-based donor (Zn-heme: ZnPP)-sensitizer ($Ru^{2+}(bpy)_3$)-acceptor (cyclic viologen: BXV^{4+}) triad **1** was used as a probe molecule. Two semisynthetic systems, Cyt-b_{562}(**1**) and Mb(**1**), in which the triad is incorporated into cytochrome b_{562} (Cyt-b_{562}) or into myoglobin (Mb), were constructed by cofactor reconstitution. These two semisynthetic proteins were compared with the triad itself (i.e., without the protein matrix) using absorption spectroscopy, steady state emission and excitation studies, laser flash photolysis experiments, and molecular modeling. Photoexcitation of the ZnPP moiety of Cyt-b_{562}(**1**) or Mb(**1**) leads to a direct ET from the triplet state of ZnPP state (^{3}ZnPP) to BXV^{4+} to generate a final charge-separated (CS) state, Cyt-$b_{562}(Zn^+)$-Ru^{2+}-$BXV^{3+\cdot}$ or Mb(Zn^+)-Ru^{2+}-$BXV^{3+\cdot}$. On the other hand, direct ET from the excited ZnPP moiety to the BXV^{4+} moiety is also involved in **1** in the absence of the protein matrix, but the excited state of ZnPP involved is not ^{3}ZnPP, but the singlet excited state (^{1}ZnPP) in this pathway. When the $Ru^{2+}(bpy)_3$ moiety of Cyt-b_{562}(**1**) or Mb(**1**) is excited, a stepwise ET relay occurs with the ion-pair, Cyt-b_{562}(Zn)-Ru^{3+}-$BXV^{3+\cdot}$ or Mb(Zn)-Ru^{3+}-$BXV^{3+\cdot}$, as an intermediate, leading to the same final CS state as that generated in the direct ET pathway. The lifetimes of the corresponding final CS states were determined to be 300 ns for **1** in the absence of the protein matrix, 600–900 ns for Cyt-b_{562}(**1**) and 1.1–18 μs for Mb(**1**), the values of which are greatly affected by the protein matrix. Molecular modeling study of the three systems consistently explained the differences of their photophysical behavior.

Keywords: artificial photosynthesis · long-lived charge separation · photoinduced electron transfer · protein matrix effect · semisynthetic system

Introduction

Effects of protein matrix on biological electron transfer processes (ET) have been actively discussed for more than one decade in the fields of chemistry and biology.[1] It is proposed that, in addition to fixed donor–acceptor distances and orientations,[2] other factors, such as the specific structural features in proteins and the dipole moments produced by a specific conformation of polypeptide chains and a hydrogen-bonding network,[3] may control biological ET. Considerable efforts gave valuable insight not only into understanding ET in biological system, but also into designing protein-based photoelectric devices.[4] However, many key questions concerning biological ET remain, for example: How does ET rate depend on distance? How do proteins ensure biological specificity in ET? Rational design and syntheses of semisynthetic systems and detailed comparison of the ET events in the presence and in the absence of the protein matrix should help to answer these questions. Nevertheless, such a comparison is rather difficult. Recently, we and other groups independently reported protein-based semisynthetic photoreaction centers as artificial photosynthetic models.[5] Covalently connected donor–acceptor dyad or triad was successfully hybridized to a protein matrix in these systems, rendering it possible to compare ET events in a protein matrix with those in a homogeneous solvent.

[a] Prof. I. Hamachi,[+] Dr. Y.-Z. Hu, H. Takashima, S. Tsukiji, Prof. S. Shinkai
Department of Chemistry and Biochemistry
Graduate School of Engineering
Kyushu University, Fukuoka 812-8581 (Japan)
Fax: (+81)92-642-3611
E-mail: itarutcm@mbox.nc.kyushu-u.ac.jp

[+] Visiting professor of the Institute of Molecular Science at Okazaki (Japan)

[b] Prof. T. Nagamune
Department of Chemistry and Biotechnology
Graduate School of Engineering, The University of Tokyo
Hongo, Bunkyo-ku, 113-8656 (Japan)

[c] Prof. S. Oishi
Department of Chemistry, School of Science
Kitasato University
Sagamihara, Kanagawa 228-8520 (Japan)

  0947-6539/00/0611-1907 $ 17.50+.50/0

In order to understand the role of protein matrix in ET within a biological system, we employed a heme-based donor (Zn-heme, ZnPP)-sensitizer ($Ru^{2+}(bpy)_3$)-acceptor (cyclic viologen, BXV^{4+}) triad **1** (ZnPP-Ru^{2+}-BXV^{4+}) as a probe molecule (Scheme 1). The $Ru^{2+}(bpy)_3$-BXV^{4+} subunit of **1** was recently described by the group of Dürr as an artificial model of the photosynthetic reaction center.[6] The $Ru^{2+}(bpy)_3$-heme subunit of **1** was demonstrated to be hybridized with apo-hemoproteins by cofactor reconstitution.[5a, b] The heme moiety of **1** is readily incorporated into the active sites of two distinct hemoproteins, cytochrome b_{562} (Cyt-b_{562}) and myoglobin (Mb), to afford two protein-based triads (Cyt-b_{562}(**1**) and Mb(**1**)). This study shows explicit experimental evidences on how protein matrix influences ET events, by comparing Cyt-b_{562}(**1**) and Mb(**1**) with the triad in the absence of a protein matrix. It was demonstrated that the ET pathways and the lifetimes of the photoinduced charge separated states (CS states) are remarkably different among these three systems.

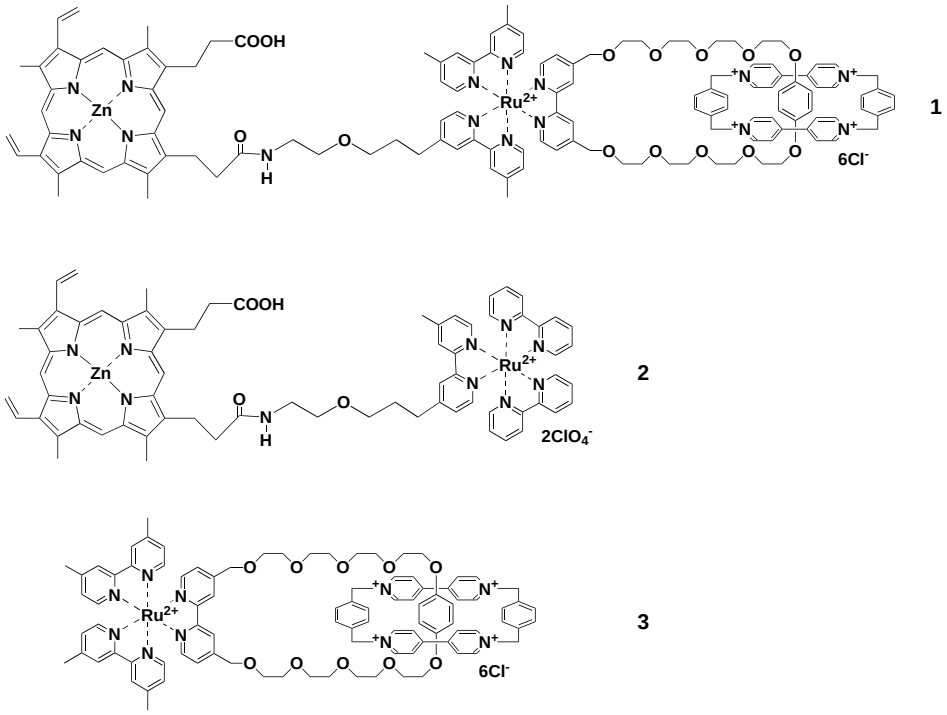

Scheme 1. Structures of the triad and the reference compounds.

Results

Reconstitution of the cofactors with apo-hemoproteins

The reconstitution of **1** and **2** with apo-Cyt-b_{562} was conducted according to the modified method reported previously for their reconstitution with apo-Mb.[7] 1.5 equiv. **1(Cl)$_6$** or **2(ClO$_4$)$_2$** dissolved in water or pyridine (**1** in water and **2** in pyridine) were added dropwise to an apo-Cyt-b_{562} solution in DMSO/H_2O (1:4 *v*/*v*) over an ice bath. The mixture was incubated at 4 °C for 6 h and then dialyzed against 10 mM phosphate buffer (pH 7.0). Purification of the mixture by gel chromatography on Sephadex G-25 afforded Cyt-b_{562}(**1**) or Cyt-b_{562}(**2**) in about 70 % yield (see Experimental Section).

Figure 1 shows the absorption spectra of **1**, Cyt-b_{562}(**1**) and Mb(**1**). The absorption spectrum of Cyt-b_{562}(**1**) is similar to that of Mb(**1**) (Figure 1),[7] which shows a sharp Soret band at 428 nm, two Q-bands at 553 nm and 596 nm, a sharp band at 284 nm (LC of $Ru^{2+}(bpy)_3$) and a shoulder at 460 nm due to the MLCT band of the $Ru^{2+}(bpy)_3$ unit. This spectrum is nearly identical to the sum of the spectra of native Zn-Cyt-b_{562} (λ_{max} = 428 nm (Soret band), 553 nm and 596 nm (Q-bands))[8] and catenane **3** (λ = 460 nm (MLCT band) and 284 nm (LC band)).[6] Spectrophotometric titration of **1** with apo-Cyt-b_{562} clearly showed 1:1 complex formation (inset of Figure 1).

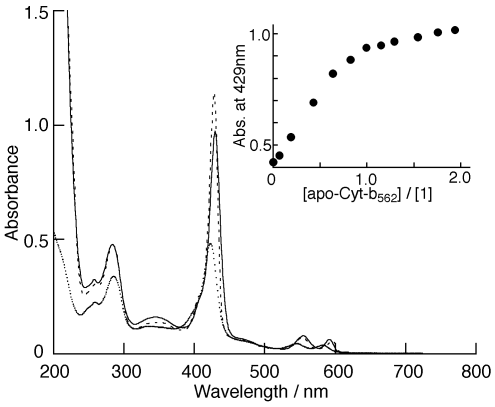

Figure 1. Absorption spectra of Cyt-b_{562}(**1**) (solid line), Mb(**1**) (dash line) and **1** (dotted line) in 50 mM phosphate buffer (pH 7.0). Inset: spectrophotometric titration curve of **1** with apo-Cyt-b_{562} in H_2O.

Abstract in Japanese:

電子移動反応における蛋白質マトリックスの効果を検討するために、ヘムとルテニウム錯体・環状ビオロゲンカテナンを基体としたトライアッド分子を二つの異なるヘム蛋白質（シトクロムb562とミオグロビン）に再構成した。得られた半合成トライアッドと蛋白質マトリックスを含まない系の電子移動特性を光化学物理、計算化学的手法で評価した。これら三つの系の直接の比較から蛋白質マトリックスによる「包み込み」によって、電荷分離状態が著しく長寿命化するだけでなく電子移動経路にも大きな影響を与えることが示された。これらの成果は人工光合成システムの構築における半合成的アプローチの有効性を如実に示している。

0947-6539/00/0611-1908 $ 17.50+.50/0 *Chem. Eur. J.* **2000**, *6*, No. 11

Similar spectral properties and titration behavior were obtained for Cyt-b_{562}(**2**). These data confirm the successful reconstitution of **1** and **2** with apo-Cyt-b_{562}. Stoichiometry and binding constants of **1** with apo-Cyt-b_{562} and apo-Mb do not display significant differences from each other, as well as their absorption spectra.

Molecular modeling

The distance and orientation between the electron donor and acceptor in a linked system are very important for ET.[2] In order to establish the geometry of **1**, Cyt-b_{562}(**1**), and Mb(**1**), molecular mechanics and molecular dynamics calculations were performed using the Discover module of Insight II. The calculated structures of **1**, Cyt-b_{562}(**1**) and Mb(**1**) in water are shown in Figure 2. In the absence of the protein matrix, the ZnPP (donor) and BXV^{4+} (acceptor) moieties in **1** tend to be close each other, leading to a U-shaped conformation, with the $Ru^{2+}(bpy)_3$ unit at the bottom and the ZnPP and BXV^{4+} moieties lying roughly in face-to-face planes. The distance between the Zn-center and the nearest N^+ of the BXV^{4+} unit is about 9 Å, which is reasonable for solvent-mediated ET between the ZnPP and BXV^{4+} units in the U-shaped conformation.[9]

As shown in Figure 2b and 2c, the ZnPP moiety in Cyt-b_{562}(**1**) and Mb(**1**), which is incorporated into the corresponding heme pocket, is separated from the $Ru^{2+}(bpy)_3$ and BXV^{4+} moieties by the protein surface. Thus the U-shaped conformation of **1** changed to more extended ones in Cyt-b_{562}(**1**) and Mb(**1**), leading to the extension of the donor (ZnPP)-acceptor (BXV^{4+}) distance. Moreover, the Cyt-b_{562} and Mb protein matrices give rise to different effects on the conformation of **1**. In Cyt-b_{562}(**1**), the connector unit between the ZnPP and $Ru^{2+}(bpy)_3$ moieties is on the outside of the protein matrix and thus is relatively flexible. Careful investigation of the conformational change of Cyt-b_{562}(**1**) showed that the BXV^{4+} and $Ru^{2+}(bpy)_3$ units approach the Cyt-b_{562} surface via electrostatic attraction with a domain of the anionic Glu and Asp residues located on N-terminal region of the helix (H_2N-Ala-*Asp*-Leu-*Glu*-*Asp*-Asn-Met-*Glu*-Thr-Leu-Asn-*Asp*-Asn-Leu-),[10] resulting in a triangle arrangement of the ZnPP, $Ru^{2+}(bpy)_3$, and BXV^{4+} moieties in the energy-minimized conformation of Cyt-b_{562}(**1**). On the other hand, the ZnPP moiety of Mb(**1**) is deeply inserted in the Mb pocket compared with Cyt-b_{562}(**1**), so that the connector between the ZnPP and $Ru^{2+}(bpy)_3$ moieties is rather rigidified by the protein matrix. In addition, the electrostatic repulsion operates between the BXV^{4+} unit and the Mb surface, since the proximity of the heme crevice of Mb is mainly surrounded with positively charged amino acid residues such as Lys, Arg, and His.[11] These factors cause further extension of the donor–acceptor distance in Mb(**1**) compared with that in Cyt-b_{562}(**1**), and result in an almost linear arrangement of the ZnPP, $Ru^{2+}(bpy)_3$, and BXV^{4+} units (Figure 2c). The distance between the Zn-center and the nearest N^+ of BXV^{4+} in Cyt-b_{562}(**1**) is estimated to be about 16 Å, whereas it is about 23 Å in Mb(**1**). Thus, the molecular modeling study clearly suggests that the protein matrix has profound effects on the donor–acceptor distance and orientation of the triad **1**, which may strongly affect the ET rates and ET pathways in **1**, Cyt-b_{562}(**1**) and Mb(**1**).

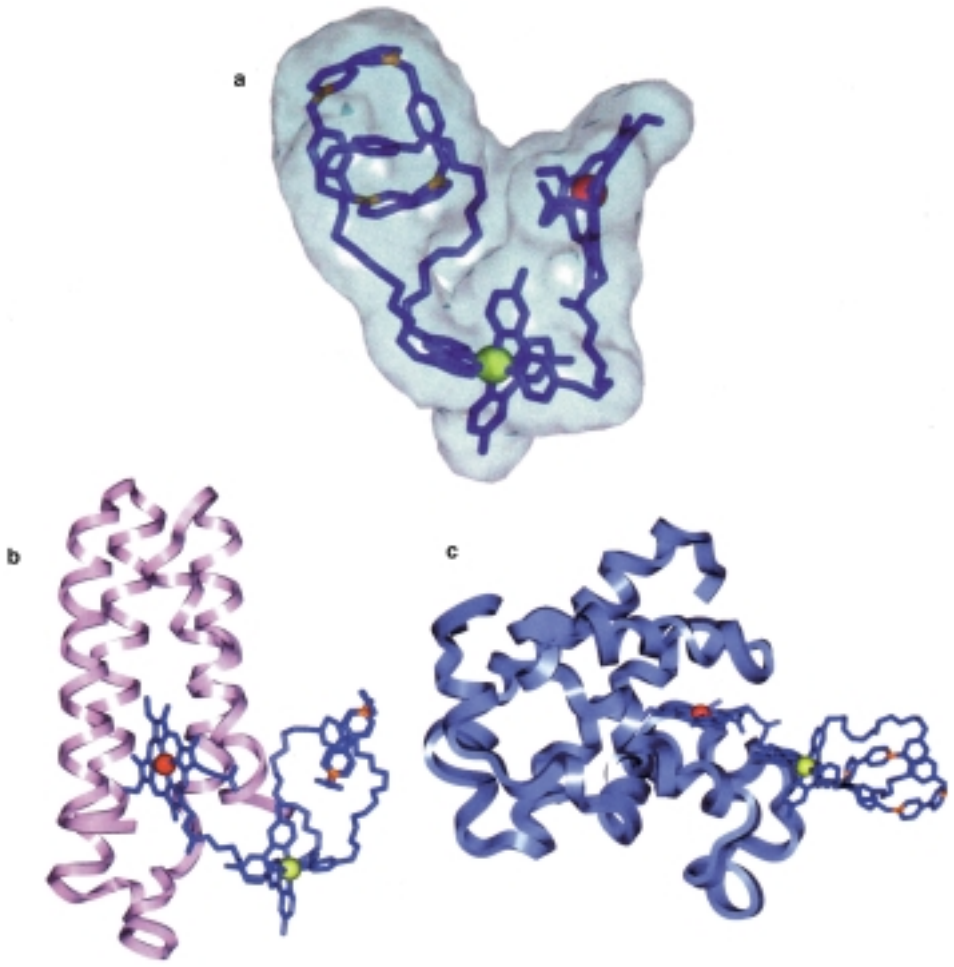

Figure 2. Energetically minimized structures by molecular modeling of a) **1**, b) Cyt-b_{562}(**1**), and c) Mb(**1**) in water. The water molecules and hydrogens were omitted for clarification.

Emission study

In the absence of the protein matrix, compound **1** exhibits very weak fluorescence with λ_{max} at 596 nm and 649 nm (shoulder), the quantum yield of which is about ten times lower than that of ZnPP (the parent) and **2**. As demonstrated

by molecular modeling, compound **1** exhibits a U-shaped conformation in water with a donor–acceptor distance of 9.3 Å, which is quite suitable for solvent-mediated ET between the terminal donor and acceptor. Thus, the quenching of the ZnPP fluorescence in **1** is attributable to the effective ET from the excited singlet state, ^{1}ZnPP, to the BXV^{4+} moiety, that is $^1ZnPP\text{-}Ru^{2+}\text{-}BXV^{4+} \rightarrow ZnPP^{+}\text{-}Ru^{2+}\text{-}BXV^{3+\bullet}$. The rate constant for this ET process is calculated to be $4.8 \times 10^9\ s^{-1}$ using Equation (1), where Φ and Φ_0 are the fluorescence quantum yield of **1** and **2**, respectively, and τ_0 is the emission lifetime of ^{1}ZnPP of **2** which was measured to be 1.8 ns by single photon counting.

$$k_{ET} = (1/\tau_0)(\Phi_0/\Phi - 1) \quad (1)$$

However, reconstitution of **1** with apo-Cyt-b_{562} and apo-Mb resulted in great recovery of the ZnPP fluorescence (Figure 3a). Fluorescence titration of **1** with apo-Cyt-b_{562} and apo-Mb (inset of Figure 3a) indicates that the fluorescence quantum yield of **1** increases dramatically with the increase of the amount of apo-protein and saturates at the ratio of 1:1 ([**1**]:[apo-protein]). These results suggest that incorporation of the heme unit of **1** into the apo-hemoprotein matrix changes the U-shaped conformation of **1** to a more extended

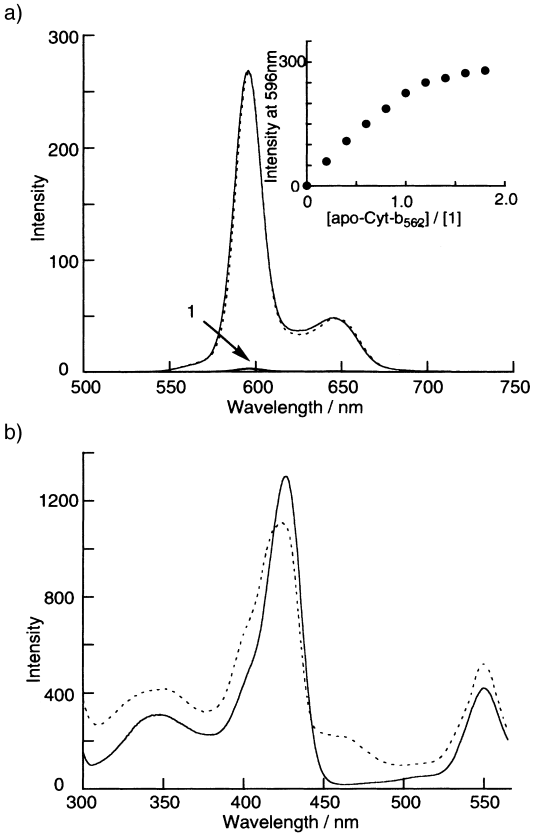

Figure 3. a) Comparison of the emission spectra of Cyt-b_{562}(**1**), Cyt-b_{562}(**2**), and compound **1** without the protein matrix in 10 mM phosphate buffer. Excitation wavelength: 428 nm. Dash line: Cyt-b_{562}(**1**); solid line: Cyt-b_{562}(**2**); dotted line: compound **1** without the protein matrix. Absorbances of the three samples at 428 nm were adjusted to the same in the measurements. b) Excitation spectra of Cyt-b_{562}(**1**) and Cyt-b_{562}(**2**) in 10 mM phosphate buffer (pH 7.0). Solid line: Cyt-b_{562}(**1**); dash line: Cyt-b_{562}(**2**). Emission wavelength detected is 596 nm.

one and thus prevents the quenching of ZnPP fluorescence by BXV^{4+}, which is consistent with the molecular modeling study. Moreover, the shapes and intensities of the emission spectra of Cyt-b_{562}(**1**) and Mb(**1**) are very similar to their control proteins, Cyt-b_{562}(**2**) and Mb(**2**), which indicates that quenching of the ZnPP fluorescence in Cyt-b_{562}(**1**) and Mb(**1**) is completely prevented (Figure 3a). Therefore, within Cyt-b_{562}(**1**) and Mb(**1**), ET from the excited singlet state of ZnPP to the $Ru^{2+}(bpy)_3$ or BXV^{4+} site can be ruled out.

We then checked the excitation spectra of Cyt-b_{562}(**1**), Mb(**1**), and their references, Cyt-b_{562}(**2**) and Mb(**2**), at emission wavelength of 596 nm. Figure 3b displays that the absorption peaks of both the ZnPP and $Ru^{2+}(bpy)_3$ units are reproduced in the excitation spectrum of Cyt-b_{562}(**2**) (428 nm and 556 nm for ZnPP and 460 nm for $Ru^{2+}(bpy)_3$); this indicates that the emission of $Ru^{2+}(bpy)_3$ is buried in the ^{1}ZnPP fluorescence spectrum (Figure 3a). However, in the case of Cyt-b_{562}(**1**), only the ZnPP absorption peaks are reproduced in the excitation spectrum. No absorption peak from the $Ru^{2+}(bpy)_3$ unit (460 nm) is observed, which implies that the $Ru^{2+}(bpy)_3$ emission is completely quenched. Similarly, the absorption peaks of both the ZnPP and $Ru^{2+}(bpy)_3$ units are observed in the excitation spectrum of Mb(**2**), whereas only the ZnPP absorption is reproduced in that of Mb(**1**). Consistently, single photon counting study showed that both emissions of Cyt-b_{562}(**2**) and Mb(**2**) decay biexponentially. The first component has a lifetime of 1.8 ns, attributable to the ^{1}ZnPP moiety, and the second one decays completely after hundreds of ns, which is due to the emission of the $Ru^{2+}(bpy)_3$ unit. However, the emissions of Cyt-b_{562}(**1**) and Mb(**1**) decay monoexponentially with the same lifetime of 1.8 ns, due to ^{1}ZnPP moiety. Quenching of the $Ru^{2+}(bpy)_3$ emission strongly supports that photoinduced ET from the excited $Ru^{2+}(bpy)_3$ to BXV^{4+} takes place in Cyt-b_{562}(**1**) and Mb(**1**), leading to the formation of the CS state, Cyt-b_{562}(Zn)-Ru^{3+}-$BXV^{3+\bullet}$ or Mb(Zn)-Ru^{3+}-$BXV^{3+\bullet}$. The one-electron oxidation potentials of ZnPP and $Ru^{2+}(bpy)_3$ are 1.06 V[2d, 12] and 1.25 V versus NHE.[6] Thus, in Cyt-b_{562}(**1**) and Mb(**1**), ET from the ZnPP moiety to $Ru^{3+}(bpy)_3$ to generate Cyt-b_{562}(Zn^+)-Ru^{2+}-$BXV^{3+\bullet}$ or Mb(Zn^+)-Ru^{2+}-$BXV^{3+\bullet}$ is expected thermodynamically favorable. The detailed mechanisms were investigated next by time-resolved laser photolysis studies.

Laser flash photolysis study

Since ET in Cyt-b_{562}(**1**) and Mb(**1**) can be initiated from both of the excited states of the ZnPP and $Ru^{2+}(bpy)_3$ moieties, the two chromophores were excited separately in the laser flash photolysis study for better clarification of the photophysical mechanisms. The excitation of the $Ru^{2+}(bpy)_3$ unit was performed at 460 nm, where more than 90% of the light is absorbed by the $Ru^{2+}(bpy)_3$ moiety (MLCT band) and less than 10% by the ZnPP moiety in Cyt-b_{562}(**1**) and Mb(**1**), whereas the ZnPP unit was excited at the Q-band of 596 nm, where the absorption of the $Ru^{2+}(bpy)_3$ unit is negligible.

Cyt-b_{562}(1): As shown in Figure 4a, pulsed laser excitation of a solution of Cyt-b_{562}(**1**) (phosphate buffer, pH 6.0) at 596 nm

0947-6539/00/0611-1910 $ 17.50+.50/0 *Chem. Eur. J.* **2000**, *6*, No. 11

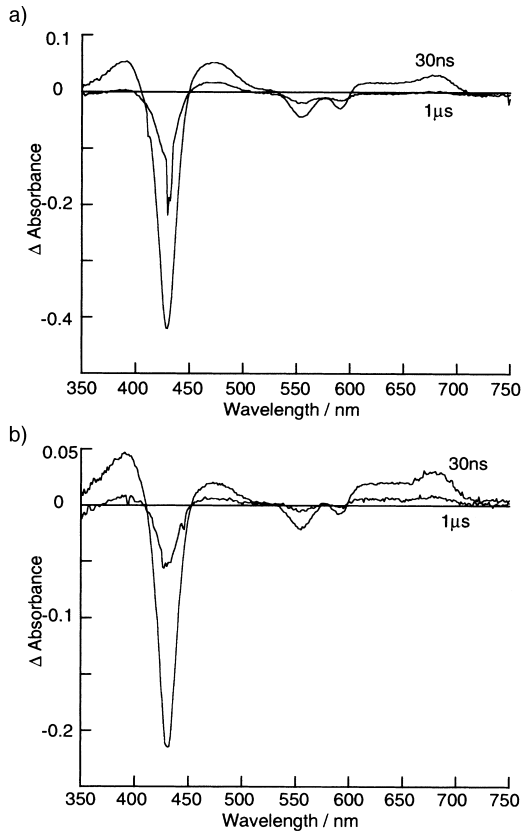

Figure 4. a) Excited state difference absorption spectra observed after laser excitation ($\lambda = 596$ nm) of Cyt-b_{562}(**1**) (8 μM) in buffer solution (pH 6.0, 50 mM phosphate) at the following delay times: 30 ns and 1 μs. The sample solutions (3 mL) were degassed with five freeze-pump-thaw cycles before the photolysis. b) Same as a) but the excitation was performed at 460 nm.

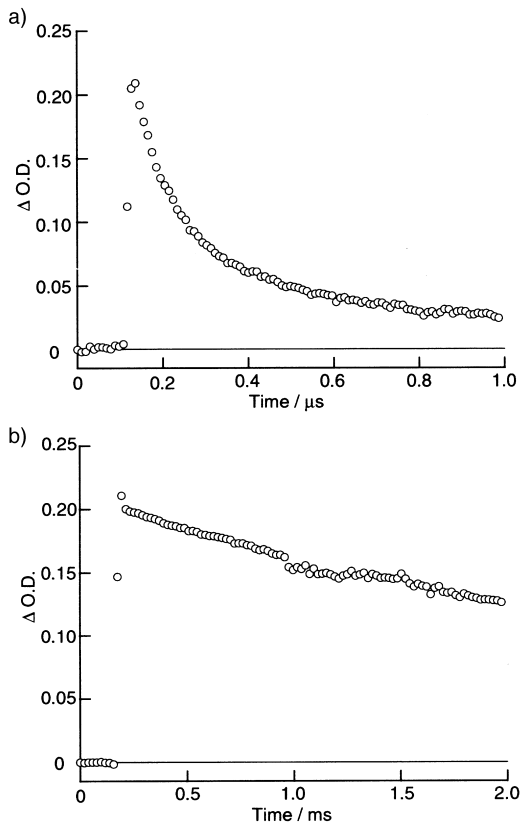

Figure 5. a) Transient kinetic trace monitored at 470 nm (^{3}ZnPP absorption) after laser flash excitation of a degassed buffer solution (pH 6.0, 50 mM phosphate) containing Cyt-b_{562}(**1**) (8.0 μM) at 596 nm. b) Transient kinetic trace monitored at 470 nm (^{3}ZnPP absorption) after laser flash excitation of a degassed buffer solution (pH 6.0, 50 mM phosphate) containing Cyt-b_{562}(**2**) (8.0 μM) at 596 nm.

leads to prompt appearances of absorption bands at 385 nm, 470 nm, 610 nm (shoulder), and 670 nm, accompanied by the bleaching of Soret and Q-bands (428 nm, 553 nm, and 596 nm). According to the literature,[2d, 12] the absorption band at 470 nm can be assigned to the excited triplet state, ^{3}ZnPP, which was populated from the excited singlet state (^{1}ZnPP) via efficient intersystem crossing. The peak at 385 nm and the shoulder at 610 nm are characteristic of the radical cation of bipyridinium salt (i.e., $BXV^{3+\bullet}$),[6] and the band centered at 670 nm is characteristic of $ZnPP^+$,[13] which partially overlaps with the absorption of the $BXV^{3+\bullet}$ radical. The appearance of $BXV^{3+\bullet}$ and $ZnPP^+$ clearly imply the formation of the CS state, that is Cyt-b_{562}(Zn^+)-Ru^{2+}-$BXV^{3+\bullet}$. The absorption bands of ^{3}ZnPP, $BXV^{3+\bullet}$, and $ZnPP^+$ species generated by excitation at 596 nm decay completely within 1 μs, concomitantly with the recovery of the Soret and Q-bands of ZnPP. Laser excitation of native Zn-Cyt-b_{562} or Cyt-b_{562}(**2**) under the same conditions simply produced the absorption of their ZnPP triplet states (^{3}Zn-Cyt-b_{562} or Cyt-b_{562}(^{3}Zn)-Ru^{2+}) and any other transient absorption was not detected.

Figure 5a shows the time course of the ^{3}ZnPP state of Cyt-b_{562}(**1**), that is Cyt-b_{562}(^{3}Zn)-Ru^{2+}-BXV^{4+}, monitored at 475 nm by excitation at 596 nm. Analysis of this curve yielded an exponential fit with a lifetime of 84 ns for Cyt-b_{562}(^{3}Zn)-Ru^{2+}-BXV^{4+}. The lifetime of Cyt-b_{562}(^{3}Zn)-Ru^{2+} was determined to be 3.0 ms from its decay curve in Figure 5b. Apparently, the decay of Cyt-b_{562}(^{3}Zn)-Ru^{2+}-BXV^{4+} is much faster than that of Cyt-b_{562}(^{3}Zn)-Ru^{2+}. Since either energy transfer or ET from ^{3}ZnPP ($E^o(ZnPP^+/{}^3ZnPP) = -0.64$ V vs. NHE) to $Ru^{2+}(bpy)_3$ is energetically unfavorable ($E^o(Ru^{2+}/Ru^+) = -1.39$ V vs. NHE),[6] the quenching of Cyt-b_{562}(^{3}Zn)-Ru^{2+}-BXV^{4+} is reasonably attributable to the direct, long-distance ET from ^{3}ZnPP to BXV^{4+}, that is Cyt-b_{562}(^{3}Zn)-Ru^{2+}-BXV^{4+} → Cyt-b_{562}(Zn^+)-Ru^{2+}-$BXV^{3+\bullet}$. The rate constant (k_{CS}) for this ET process is calculated to be 1.1×10^7 s^{-1} using Equation (2), where τ and τ_o are the lifetimes of Cyt-b_{562}(^{3}Zn)-Ru^{2+}-BXV^{4+} and Cyt-b_{562}(^{3}Zn)-Ru^{2+}.

$$k_{CS} = 1/\tau - 1/\tau_o \quad (2)$$

The kinetic behavior of the CS state, Cyt-b_{562}(Zn^+)-Ru^{2+}-$BXV^{3+\bullet}$, were monitored at 670 nm. The time course generated by excitation at the Q-band (596 nm) shows that the rise of transient absorption at 670 nm is not "instantaneous" but instead grows in on a rather slow time scale and then decays subsequently within 1 μs (Figure 6a). This kinetic behavior is consistent with a typical consecutive reaction (A → B → C),[14] in which A would correspond to Cyt-b_{562}(^{3}Zn)-Ru^{2+}-BXV^{4+}, B, to Cyt-b_{562}(Zn^+)-Ru^{2+}-$BXV^{3+\bullet}$, and C, to the initial ground state Cyt-b_{562}(Zn)-Ru^{2+}-BXV^{4+}. A nonlinear

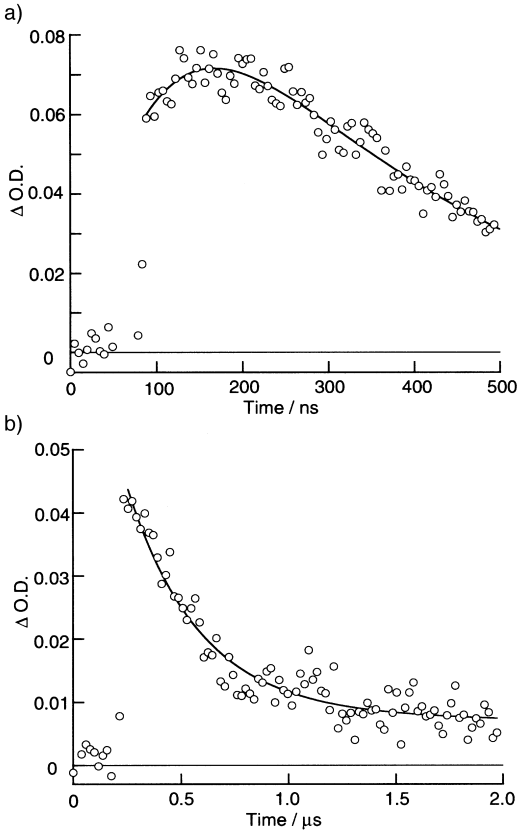

Figure 6. a) Kinetic trace monitored at 670 nm, which was produced by laser flash photolysis of a degassed buffer solution (pH 6.0, 50 mM phosphate) containing Cyt-b_{562}(**1**) (8.0 μM) at 596 nm. b) Same as a) but the excitation wavelength used was 460 nm. The fitting curves in a) and b) are given by the solid lines.

least-squares fit of the data (solid line) yielded a rate constant (k_{CS}) of $2.3 \times 10^7\ s^{-1}$ for the charge separation (CS) process, Cyt-b_{562}(^{3}Zn)-Ru^{2+}-BXV^{4+} → Cyt-b_{562}(Zn^+)-Ru^{2+}-$BXV^{3+\bullet}$, and a rate constant (k_{CR}) of $2.8 \times 10^6\ s^{-1}$ for the charge recombination (CR) process, Cyt-b_{562}(Zn^+)-Ru^{2+}-$BXV^{3+\bullet}$ → Cyt-b_{562}(Zn)-Ru^{2+}-BXV^{4+}. The rate constant of k_{CS} is in good agreement with that obtained from the decay of ZnPP triplet state.

When the Ru^{2+}(bpy)$_3$ moiety of Cyt-b_{562}(**1**) was selected to excite at 460 nm, ^{3}ZnPP, $BXV^{3+\bullet}$, and $ZnPP^+$ species were also formed promptly, but the efficiency of the formation of ^{3}ZnPP was much lower than that excited at 596 nm (Figure 4b). The appearance of the ^{3}ZnPP absorption is due to the weak light absorption by the ZnPP moiety at 460 nm, and its decay behavior is very similar to that generated by excitation at 596 nm (Figure 5a). However, the transient kinetics monitored at 670 nm (Figure 6b) exhibits a quite different profile from that in Figure 6a. It shows that the CS state, Cyt-b_{562}(Zn^+)-Ru^{2+}-$BXV^{3+\bullet}$, is formed "instantaneously" after the laser flash and then decays with a rate constant quite close to that measured from Figure 6a. The rate for the formation of the absorption at 670 nm is faster than our instrument resolution (fwhm = 5 ns, i.e., both k_{CS1} and $k_{CSH} > 2 \times 10^8\ s^{-1}$, CSH: charge shift). This rate is over 20 times faster than the decay of Cyt-b_{562}(^{3}Zn)-Ru^{2+}-BXV^{4+} ($\tau = 84$ ns), which indicates that the contribution of the direct ET pathway, that is Cyt-b_{562}(^{3}Zn)-Ru^{2+}-BXV^{4+} → Cyt-b_{562}(Zn^+)-Ru^{2+}-$BXV^{3+\bullet}$, to the formation of the CS state is negligible in the case of excitation at 460 nm. Therefore, it is reasonably concluded that the CS state is generated via the stepwise ET route, that is Cyt-b_{562}(Zn)-*Ru^{2+}-BXV^{4+} → Cyt-b_{562}(Zn)-Ru^{3+}-$BXV^{3+\bullet}$ → Cyt-b_{562}(Zn^+)-Ru^{2+}-$BXV^{3+\bullet}$, the rate constants of which are both faster than $2 \times 10^8\ s^{-1}$. Analysis of the decay curve yields an exponential fit with a lifetime of 606 ns, which leads to a rate constant k_{CR} for the back ET of $1.7 \times 10^6\ s^{-1}$. The rate constant is in good agreement with the k_{CR} obtained by excitation at 596 nm (see above).

The rate constants for the direct ET from ^{3}ZnPP to BXV^{4+} (k_{CS}) and the subsequent charge recombination of the CS state (k_{CR}) in Cyt-b_{562}(**1**) are pH dependent in the range of pH 4.0 – 6.0 (Table 1). Decrease of pH value results in gradual decreases in k_{CS} and k_{CR}.

The quantum yield of Cyt-b_{562}(Zn^+)-Ru^{2+}-$BXV^{3+\bullet}$ was determined by a comparative method based on the extinction coefficients of the triplet state of TPP[15] and Cyt-b_{562}(Zn^+)-Ru^{2+}-$BXV^{3+\bullet}$ ($\varepsilon_{670\,nm} = 17000\ cm^{-1}M^{-1}$). Since the CS state can be formed via two different ET pathways, that is direct ET from ^{3}ZnPP to BXV^{4+} and stepwise ET relay initiated from the excited state of the Ru^{2+}(bpy)$_3$ unit, the quantum yield was measured by excitation at different wavelengths. When excited at 460 nm (MLCT band of Ru^{2+}(bpy)$_3$), the quantum yield for the formation of Cyt-b_{562}(Zn^+)-Ru^{2+}-$BXV^{3+\bullet}$ via the stepwise ET relay was measured to be 0.33, whereas the quantum yield via the direct ET pathway was determined to be 0.38 by excitation at 596 nm.

Table 1. Summary of the distances[a] and photophysical properties in the CS and CR process.

	Distance [Å]	pH	Rates of CS[b]	Lifetimes (rates) of CR[b]
		4.0	$3.3 \times 10^6\ s^{-1}$	990 ns ($1.0 \times 10^6\ s^{-1}$)
Cyt-b_{562}(**1**)	16.3	5.0	$7.0 \times 10^6\ s^{-1}$	769 ns ($1.3 \times 10^6\ s^{-1}$)
		6.0	$1.2 \times 10^7\ s^{-1}$	606 ns ($1.7 \times 10^6\ s^{-1}$)
			$4.7 \times 10^5\ s^{-1}$ (70 %)[c]	1.1 μs ($9.2 \times 10^5\ s^{-1}$) (75 %)[c]
Mb(**1**)	22.9	6.0 – 8.0	$5.0 \times 10^4\ s^{-1}$ (30 %)[c]	18.4 μs ($5.4 \times 10^4\ s^{-1}$) (25 %)[c]
1	9.3	–	$4.8 \times 10^9\ s^{-1}$[d]	300 ns ($3.3 \times 10^6\ s^{-1}$)[e]

[a] These values were estimated by the distance between Zn center and the nearest N^+ of BXV^{4+}. [b] These values were determined by the decay of ^{3}ZnPP for CS and $ZnPP^+$ for CR upon photoirradiation at 596 nm, respectively. All calculated values included experimental error within ± 14 %. [c] Kinetic traces were analyzed by biexponential fitting. These values represent the contribution of the corresponding kinetic components. [d] This rate constant was estimated from the singlet (^{1}ZnPP) ET by the emission study. [e] Excitation at 460 nm yielded very similar results.

Mb(1): When Mb(**1**) was excited by pulsed laser flash at 460 nm or 596 nm, transient absorption spectra consisting of absorption bands of $BXV^{3+\bullet}$ (385 nm and 610 nm), ^{3}ZnPP (470 nm), and $ZnPP^+$ (670 nm) were produced promptly, which are very similar to those shown in Figure 4. These

0947-6539/00/0611-1912 $ 17.50+.50/0 *Chem. Eur. J.* **2000**, *6*, No. 11

changes clearly imply the appearances of the CS state, Mb(Zn^+)-Ru^{2+}-$BXV^{3+\bullet}$, and the triplet state, Mb(^3Zn)-Ru^{2+}-BXV^{4+}. Laser excitation of Zn-Mb or Mb(Zn)-Ru^{2+} under the same conditions simply produced the absorption of their ZnPP triplet states (^{3}Zn-Mb or Mb(^3Zn)-Ru^{2+}) and any other transient absorption was not detected.

The lifetime of Mb(^3Zn)-Ru^{2+} was determined to be 3.9 ms by monitoring the decay at 470 nm, whereas Mb(^3Zn)-Ru^{2+}-BXV^{4+} decays biexponentially with lifetimes of 2.1 μs (70%) and 19.8 μs (30%) (Figure 7a). Apparently, the decay of Mb(^3Zn)-Ru^{2+}-BXV^{4+} is much faster than that of Mb(^3Zn)-Ru^{2+}, which suggests the occurrence of the direct, long-distance ET from ^{3}ZnPP to BXV^{4+}, that is Mb(^3Zn)-Ru^{2+}-BXV^{4+} → Mb(Zn^+)-Ru^{2+}-$BXV^{3+\bullet}$. The rate constants for this ET process were calculated to be $4.7 \times 10^5\ s^{-1}$ and $5.0 \times 10^4\ s^{-1}$ using the lifetimes of Mb(^3Zn)-Ru^{2+}-BXV^{4+} and Mb(^3Zn)-Ru^{2+}, which are much slower than that of Cyt-b_{562}(**1**) (see above). Similar to the case of Cyt-b_{562}(**1**), when Mb(**1**) was excited at 596 nm, the transient kinetic behavior at 670 nm (Figure 7b) exhibits a slow rising and slow decay profile, which is consistent with a typical consecutive reaction (A → B → C). A would correspond to Mb(^3Zn)-Ru^{2+}-BXV^{4+}, B, to Mb(Zn^+)-Ru^{2+}-$BXV^{3+\bullet}$, and C, to the initial ground state Mb(Zn)-Ru^{2+}-BXV^{4+}. A nonlinear least-squares fit of the data (solid line) yielded rate constants (k_{CS}) of $7.6 \times 10^5\ s^{-1}$ (70%) and $5.0 \times 10^4\ s^{-1}$ (30%) for the process, Mb(^3Zn)-Ru^{2+}-BXV^{4+} → Mb(Zn^+)-Ru^{2+}-$BXV^{3+\bullet}$, and rate constants (k_{CR}) of $1.1 \times 10^6\ s^{-1}$ (70%) and $5.0 \times 10^4\ s^{-1}$ (30%) for the process, Mb(Zn^+)-Ru^{2+}-$BXV^{3+\bullet}$ → Mb(Zn)-Ru^{2+}-BXV^{4+}. The constants of k_{CS} are in good agreement with those obtained from the decay of Mb(^3Zn)-Ru^{2+}-BXV^{4+}.

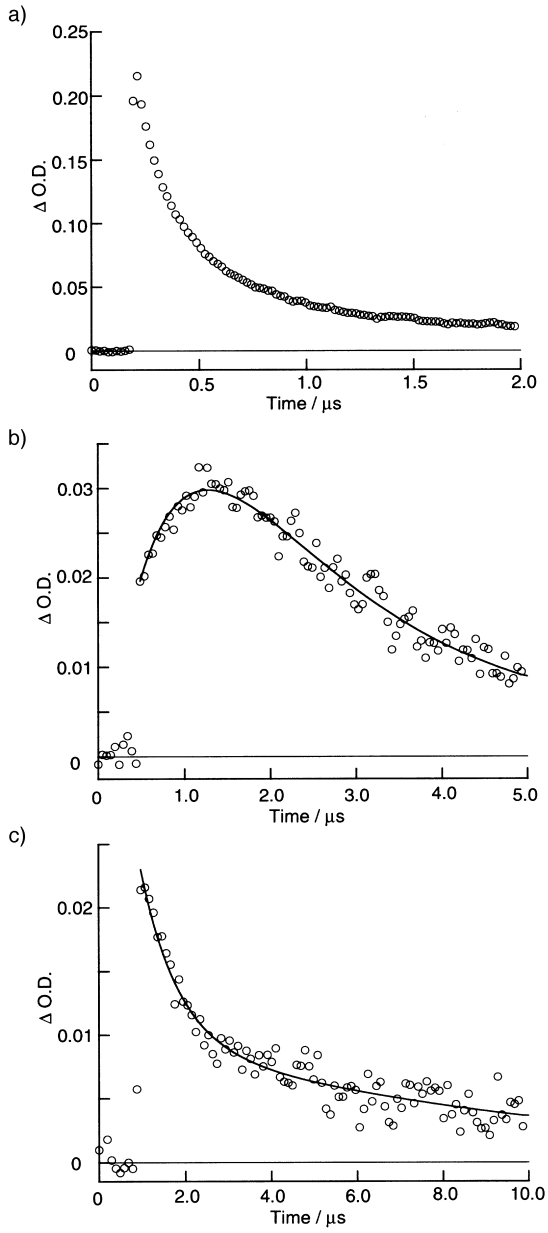

Figure 7. Transient kinetics of Mb(**1**) produced by 596 nm and 460 nm laser excitation of a degassed buffer solution (pH 7.0, 50 mM phosphate) containing Mb(**1**) (8.0 μM). a) Kinetic trace monitored at 470 nm (^{3}ZnPP absorption) by excitation at 596 nm. b) Kinetic trace monitored at 670 nm by excitation at 596 nm. c) Kinetic trace monitored at 670 nm by excitation at 460 nm. The fitting curves are given by the solid lines.

Figure 7c shows the transient kinetics at 670 nm generated by excitation of Mb(**1**) at 460 nm, which exhibits much different kinetic behavior from that in Figure 7b. The transient absorption was formed "instantaneously" with a rate faster than our instrument resolution (fwhm = 5 ns, i.e., both k_{CS1} and $k_{CSH} > 2 \times 10^8\ s^{-1}$). Since this rate is over 500 times faster than the rate of the direct ET initiated by Mb(^3Zn)-Ru^{2+}-BXV^{4+} ($k_{CS} = 4.8 \times 10^5\ s^{-1}$), it is reasonably concluded that the CS state is generated via the stepwise ET route, that is Mb(Zn)-*Ru^{2+}-BXV^{4+} → Mb(Zn)-Ru^{3+}-$BXV^{3+\bullet}$ → Mb(Zn^+)-Ru^{2+}-$BXV^{3+\bullet}$, the rate constants of which are both faster than $2 \times 10^8\ s^{-1}$. Analysis of the decay curve yields a biexponential fit with lifetimes of 1.1 μs (75%) and 18.4 μs (25%), which lead to rate constants k_{CR} for the back ET of $9.2 \times 10^5\ s^{-1}$ and $5.4 \times 10^4\ s^{-1}$. These rate constants are consistent with the k_{CR} obtained by excitation at 596 nm.

It was found that, in contrast to the case of Cyt-b_{562}(**1**), change of pH has no obvious effect on the direct ET from ^{3}ZnPP to BXV^{4+} and the charge recombination of the CS state in Mb(**1**). The quantum yield for the formation of Mb(Zn^+)-Ru^{2+}-$BXV^{3+\bullet}$ via the stepwise ET pathway was determined to be 0.08 by excitation at 460 nm, and that via the direct ET pathway is 0.16 by excitation at 596 nm.

Compound 1 in the absence of protein matrix: As demonstrated by the fluorescence study, rapid singlet ET from ^{1}ZnPP to BXV^{4+} takes place in **1** in the absence of the protein matrix ($k_{CS} = 4.8 \times 10^9\ s^{-1}$). Consistently, pulsed laser excitation of **1** at 596 nm in the absence of the protein matrix results in prompt appearances of the absorption bands of $BXV^{3+\bullet}$ (390 nm and 610 nm) and $ZnPP^+$ (670 nm) and the bleaching of the Soret and Q-bands, which suggests the formation of the CS state, $ZnPP^+$-Ru^{2+}-$BXV^{3+\bullet}$ (Figure 8a). Any transient absorption due to the ZnPP triplet state (^{3}ZnPP) was not observed; this indicates that the intersystem crossing from ^{1}ZnPP to ^{3}ZnPP is completely inhibited in **1**. The CS state, $ZnPP^+$-Ru^{2+}-$BXV^{3+\bullet}$, is generated by the direct ET from the excited singlet state of the ZnPP unit (^{1}ZnPP) to the BXV^{4+} unit, which agrees well with the emission study. Fitting the decay curve of $ZnPP^+$-Ru^{2+}-$BXV^{3+\bullet}$ (Figure 8b) yielded a lifetime of 300 ns, which is relatively shorter than that of

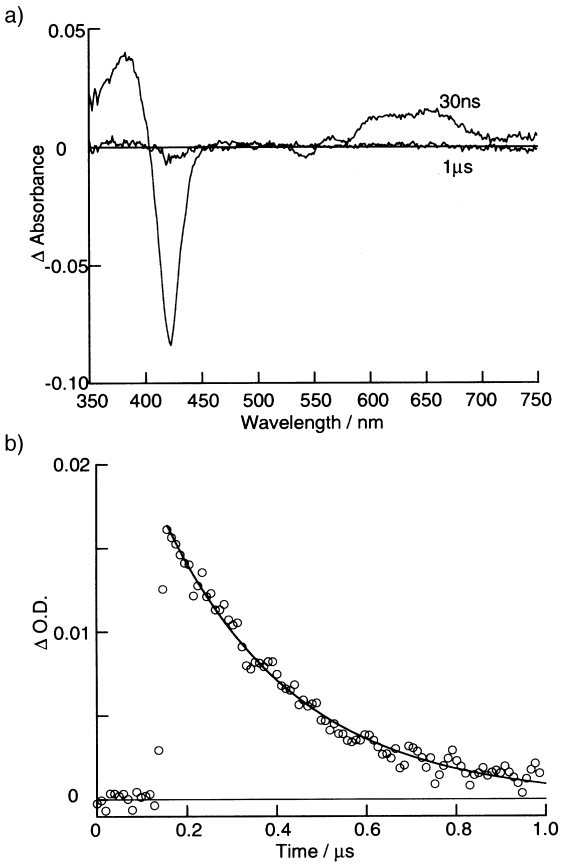

Figure 8. a) Excited state difference absorption spectra observed after laser excitation ($\lambda = 596$ nm) of **1** in water in the abscence of the protein matrix at delay times of 30 ns and 1 μs. b) Kinetic trace monitored at 670 nm produced by laser photolysis of **1** in the abscence of the protein matrix. The fitting curve is given by the solid line.

Cyt-b_{562}(Zn^{+})-Ru^{2+}-$BXV^{3+\cdot}$ (pH 6.0) and is much shorter than that of Mb(Zn^{+})-Ru^{2+}-$BXV^{3+\cdot}$. Laser excitation of **1** at 460 nm yielded very similar results. Since both the ZnPP and $Ru^{2+}(bpy)_3$ units of **1** exhibit strong absorption at 460 nm, the stepwise ET pathway can not be separated from the direct ET pathway in the case of **1** without the protein matrix. The quantum yield of $ZnPP^{+}$-Ru^{2+}-$BXV^{3+\cdot}$ was measured to be 0.26 by excitation at 596 nm.

Discussion

On the basis of the fluorescence and laser flash photolysis studies, the reaction scheme of Cyt-b_{562}(**1**) and Mb(**1**) can be written as shown in Scheme 2, and the reaction scheme for **1** in the absence of a protein matrix is shown in Scheme 3.[16] Scheme 2 shows that, when the $Ru^{2+}(bpy)_3$ moiety of Cyt-b_{562}(**1**) or Mb(**1**) is excited, a stepwise ET relay mechanism occurs with the intermediate ion-pair, Cyt-b_{562}(Zn)-Ru^{3+}-$BXV^{3+\cdot}$ or Mb(Zn)-Ru^{3+}-$BXV^{3+\cdot}$, as a real intermediate. On the other hand, excitation of the ZnPP moiety of Cyt-b_{562}(**1**) or Mb(**1**) leads to direct ET from the ^{3}ZnPP state to BXV^{4+}. Both of these ET pathways finally generate the same CS state, Cyt-b_{562}(Zn^{+})-Ru^{2+}-$BXV^{3+\cdot}$ or Mb(Zn^{+})-Ru^{2+}-$BXV^{3+\cdot}$. Direct ET from the excited ZnPP moiety to the BXV^{4+} moiety is also involved in **1** in the absence of the protein matrix (Scheme 3), but the excited state of ZnPP involved in this pathway is ^{1}ZnPP, but not ^{3}ZnPP.

The donor–acceptor distances and rate constants for the direct ET and charge recombination in compound **1**, Cyt-b_{562}(**1**), and Mb(**1**) are summarized in Table 1. We failed to determine the rate constants for the stepwise ET in the systems studied due to instrumental limitation. However,

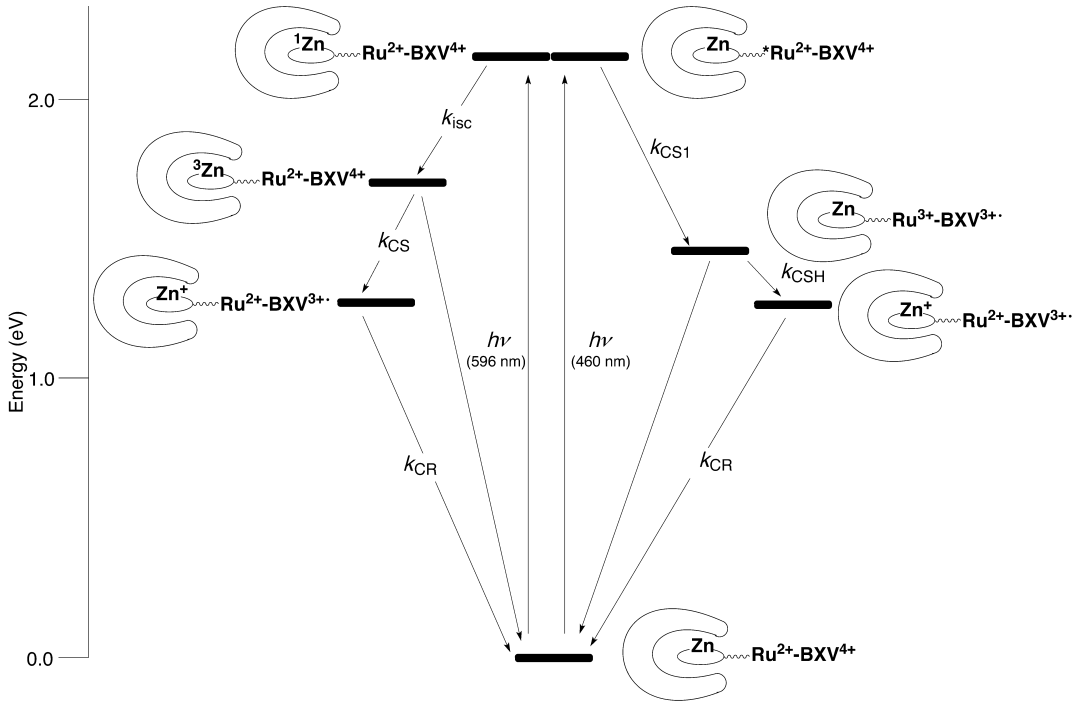

Scheme 2. Photoreaction scheme of Cyt-b_{562}(**1**) and Mb(**1**).

0947-6539/00/0611-1914 $ 17.50+.50/0 *Chem. Eur. J.* **2000**, *6*, No. 11

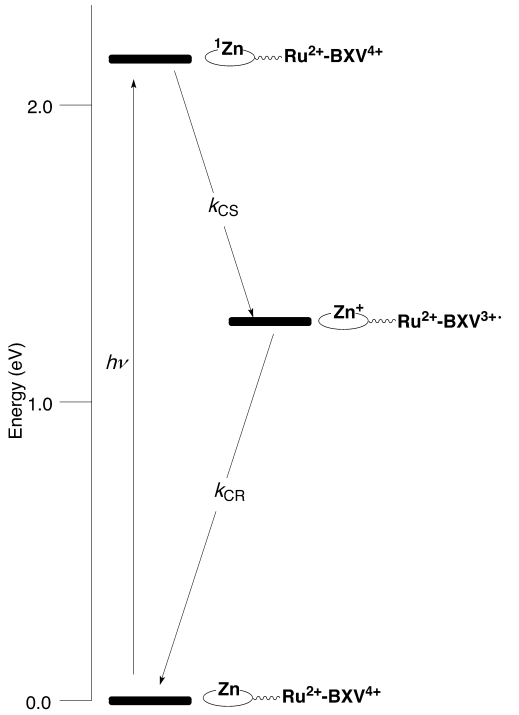

Scheme 3. Photoreaction scheme of **1** in the abscence of protein matrix. Since we have not any direct evidence for the stepwise ET pathway initiated from the $Ru^{2+}(bpy)_3$ excited state, it is not shown in this scheme.

Table 1 clearly shows that partial incorporation of **1** into hemoproteins has profound effects on the direct ET from ZnPP to BXV^{4+} and charge recombination of the CS states. Similar observations were recently addressed by Willner and co-workers.[5h] As demonstrated in the molecular modeling study, compound **1** exhibits a thermodynamically favorable U-shaped conformation with the terminal ZnPP and BXV^{4+} moieties close to each other, which facilitates a solvent-mediated ET between the two moieties.[9] As a result, the excited singlet state of the ZnPP moiety (^{1}ZnPP) in **1** is efficiently quenched by the rapid ET pathway of ^{1}ZnPP-Ru^{2+}-BXV^{4+} → $ZnPP^+$-Ru^{2+}-$BXV^{3+\cdot}$ (k_{CS} in Scheme 3). The intersystem crossing (k_{ISC}) from ^{1}ZnPP to ^{3}ZnPP in **1** is also completely prevented, since no ^{3}ZnPP absorption was observed upon laser excitation of **1** in the absence of protein matrix (Figure 8a). On the other hand, molecular modeling study clearly shows that, when the ZnPP unit of **1** is incorporated into apo-Cyt-b_{562} or apo-Mb, the U-shaped conformation of **1** is changed to a more extended one, which results in large increase in donor–acceptor distance (Table 1). The extension of the donor–acceptor distances in Cyt-b_{562}(**1**) and Mb(**1**) gives rise to great recovery of the ^{1}ZnPP fluorescence and inhibits the direct ET from ^{1}ZnPP to BXV^{4+}; this leads to efficient intersystem crossing from ^{1}ZnPP to ^{3}ZnPP. Thus, when the ZnPP unit of Cyt-b_{562}(**1**) or Mb(**1**) is excited, the direct ET pathway is regulated to proceed from ^{3}ZnPP to BXV^{4+} with a relatively slow rate constant (see Table 1).

Since the isoelectric point of Cyt-b_{562} is about pH 5.0,[17] its surface is negatively charged at neutral pH. More importantly, an anionic cluster consisting of repeated Glu and Asp residues is located on the proximity of the outside of the heme crevice. Molecular modeling study indicates that the BXV^{4+} and $Ru^{2+}(bpy)_3$ units of Cyt-b_{562}(**1**) tend to approximate to the protein surface via electrostatic interaction with the anionic cluster, and the flexibly connected ZnPP, $Ru^{2+}(bpy)_3$, and BXV^{4+} units adopt a triangle conformation. However, in Mb(**1**), the deeper insertion of the ZnPP moiety into Mb rigidifies the connector between the ZnPP and $Ru^{2+}(bpy)_3$ moieties by the protein matrix, which leads to large extension of the donor–acceptor distance with respect to that of Cyt-b_{562}(**1**). In addition, since the exterior surface of the heme crevice of Mb is positively charged at neutral pH,[11] the donor–acceptor distance in Mb(**1**) might be further extended by the electrostatic repulsion between the BXV^{4+} unit and Mb surface. Therefore, the difference in interactions between the protein matrices and BXV^{4+} in Cyt-b_{562}(**1**) and Mb(**1**) strongly affects the donor–acceptor distances, orientations, and thus the rate constants for charge separations and charge recombinations. As demonstrated by the laser flash photolysis study, at neutral pH, the rate constant for the ET from ^{3}ZnPP to BXV^{4+} (k_{CS}) in Mb(**1**) is about 20 times slower than that in Cyt-b_{562}(**1**) (Table 1). Moreover, the CS state of Mb(**1**), $Mb(Zn^+)$-Ru^{2+}-$BXV^{3+\cdot}$, is about 2–30 times longer-lived than Cyt-$b_{562}(Zn^+)$-Ru^{2+}-$BXV^{3+\cdot}$. Thus, it is clear that, in our systems, spatial arrangements of the donor and acceptor, such as donor–acceptor distances and orientations, play major roles in controlling the both processes; this suggests that these ET proceed mainly via a through-space mechanism, althouth a through-bond ET mechanism may also be involved.

In the pH range around the pI of Cyt-b_{562} (pH 4.0–6.0), the rate constants for the direct ET (k_{CS}), and charge recombination (k_{CR}) in Cyt-b_{562}(**1**) are pH dependent. The k_{CS} and k_{CR} at pH 6.0 are faster than those at pH 4.0. The decreases in k_{CS} and k_{CR} at pH lower than pI of Cyt-b_{562} (pI 5.0) reflect that the electrostatic interactions between the BXV^{4+} unit and the protein surface are lessened with the protonation of the protein surface, and thus the donor–acceptor distance is extended with the decrease of pH. In contrast to the case of Cyt-b_{562}(**1**), change of pH in the range around the pI of Mb (pH 6.0–8.0) has no obvious effect on the k_{CS} and k_{CR} of Mb(**1**), which indicates that the donor–acceptor distance in Mb(**1**) can not be affected significantly in this pH range.

In summary, our study clearly demonstrated that protein matrix plays crucial roles in biological ET, including i) isolation of the redox partners in a multicomponent assembly to prevent their stacking in the ground state, ii) fixation of the conformation of a chromophore, depending on interactions between the chromophore and the protein surface, iii) regulation of the ET pathway among singlet ET, triplet ET, a short-cut process and a stepwise process, and iv) control of the lifetime of a resultant charge-separated state. We are convinced that these effects are useful for advancing artificial photoreaction systems.

Experimental Section

The syntheses of compounds **1** and **2** have been reported previously.[7] Other chemicals were used without further purification.

Reconstitution of apo-Cyt-b_{562} with Zn-heme derivatives:[18] The apo-Cyt-b_{562} was prepared by the similar method of Mb. The reconstitution was conducted to the modified method reported previously by us. 1.5 equiv. of

the cofactor dissolved in water or pyridine (**1** in water, ZnPP and **2** in pyridine) were added dropwise to an apo-Cyt-b_{562} solution in distilled water and DMSO over an ice bath. The ratio of the organic solvent in the final component was adjusted to be 20% (*v*/*v*). The mixture was incubated at 4°C for 6 h and then dialyzed against distilled water three times and phosphate buffer (pH 7.0) twice. After filtration through a cellulose membrane ($\phi = 0.20\,\mu$m), the clear supernatant was applied to gel chromatography on Sephadex G-25 (eluent: 10 mM phosphate buffer, pH 7.0). The purified Cyt-b_{562} solutions were concentrated by ultrafiltration (amicon, YM 10 membrane). All of the semisynthetic Cyt-b_{562} proteins were obtained in yields of the range of 55–75%, which were determined spectrophotometrically.

Fluorescence measurements: The fluorescence and excitation spectra were recorded on 10^{-6} M solutions with Hitachi F-4500 fluorescence photometer. The fluorescence lifetimes were measured with a sub-nanosecond time-correlated single photon counting system (PTI-3000, excitation at 430 nm, and monitored at 600 nm). The sample solutions were degassed with five freeze-pump-thaw cycles before the measurements. The experimental error of the lifetime values was estimated to be within 10%.

Laser photolysis experiments: The sample solutions (3 mL) degassed with five freeze-pump-thaw cycles were subjected to pulsed laser photolysis at 20°C, using a third harmonic light (460 nm or 596 nm, fwhm = 5 ns) from a Q-switched Nd/YAG laser (Quanta-Ray DCR-11) for excitation equipped with the optical parametric oscillator (OPO). A right-angle optical system was employed for the excitation-analysis setup. Probe lights were detected by a photomultiplier tube (Hamaphoto R 446) or a photodiode array (Princeton IRY-1024 G/RB, gate width = 4 ns). 100 flashes were set for each measurement to determine the experimental error.

Determination of quantum yields: The quantum yields of the CS states were determined by a comparative method based on the extinction coefficients of the triplet state of meso-tetraphenyl porphyrin (790 nm) and the CS states (670 nm).[15]

Molecular modeling: Model buildings and molecular dynamics calculations were performed with Insight II/Discover 98 packaged in the context of the Molecular Simulations Inc. (MSI). All calculations were performed with the extensive systematic force field (ESFF). The triad molecule **1** was first constructed with Builder module of the Insight package. Initial calculation was carried out in vacuo by molecular mechanics (MM), followed by molecular dynamics (MD) minimization around 500 K. Some of the conformations which were energetically stabilized was chosen for next solvation analysis. The triad molecule **1** solvated on the surface of five layers of water was used for the next MM calculations. The distance between zinc and nitrogen of BXV^{4+} was estimated from this final minimized structure. Reconstruction of our semisynthetic Mb or Cyt-b_{562} was performed using Biopolymer modules based on the X-ray crystallographic data of Mb and Cyt-b_{562} in RSCB protein data bank (PDB), followed by replacement of the metal center from iron to zinc and adjustment of the coordination sphere of ZnPP. This semisynthetic protein was treated as an assembled molecule in a waterbox, followed by MM and MD calculations with the gradient minimization in a procedure similar to the case of the triad **1**.

Acknowledgement

Y.Z.H. is a postdoctoral fellow of the Japan Society for the Promotion of Science (JSPS), and H.T. and S.T. are JSPS fellows for Japanese Junior Scientists. We are grateful to Dr. H. Ishida (Inoue Photochrogenesis Project, ERATO) for valuable comments on molecular modeling study. We thank Prof. S. Sligar for his kind gift of TB-1 cells harboring the pNS207 plasmid. This research was partially supported by a specially promoted area (Biotargeting, No. 11132261) and a COE formation program (Molecular Assembly) from the Ministry of Education, Science, Sports and Culture of Japan.

[1] a) R. A. Marcus, N. Sutin, *Biochim. Biophys. Acta* **1985**, *811*, 265; b) G. McLendon, *Acc. Chem. Res.* **1988**, *21*, 160; c) J. R. Winkler, H. B. Gray, *Chem. Rev.* **1992**, *92*, 369; d) S. S. Isied, M. Y. Ogawa, J. F. Wishart, *Chem. Rev.* **1992**, *92*, 381; e) C. C. Moser, C. C. Page, R. Farid, P. L. Dutton, *J. Bioenerg. Biomembr.* **1995**, *27*, 263.

[2] a) H. B. Gray, B. G. Malmström, *Biochemistry* **1989**, *19*, 7499; b) D. N. Beratan, J. N. Betts, J. N. Onuchic, *Science* **1991**, *252*, 1285; c) S. S. Skourtis, J. J. Regan, J. N. Onuchic, *J. Phys. Chem.* **1994**, *98*, 3379; d) A. W. Axup, M. Albin, S. L. Mayo, R. J. Crutchley, H. B. Gray, *J. Am. Chem. Soc.* **1988**, *110*, 435; e) D. R. Casimiro, L.-L. Wong, J. L. Colön, T. E. Zewert, J. H. Richards, I.-J. Chang, J. R. Winkler, H. B. Gray, *J. Am. Chem. Soc.* **1993**, *115*, 1485.

[3] a) D. S. Wuttke, M. J. Bjerrum, J. R. Winkler, H. B. Gray, *Science* **1992**, *256*, 1007; b) C. C. Moser, J. M. Keske, K. Warncke, R. S. Rarid, P. L. Dutton, *Nature* **1992**, *355*, 796; c) E. Galoppini, M. A. Fox, *J. Am. Chem. Soc.* **1996**, *118*, 2299.

[4] a) I. Willner, E. Zahavy, *Angew. Chem.* **1994**, *106*, 594; *Angew. Chem. Int. Ed. Engl.* **1994**, *33*, 581; b) E. Katz, V. Heleg-Shabtai, I. Willner, H. K. Rau, W. Haehnel, *Angew. Chem.* **1998**, *110*, 3443; *Angew. Chem. Int. Ed.* **1998**, *37*, 3253; c) I. Willner, V. Heleg-Shabtai, E. Katz, H. K. Rau, W. Haehnel, *J. Am. Chem. Soc.* **1999**, *121*, 6455; d) L.-H. Guo, S. Mukamel, G. McLendon, *J. Am. Chem. Soc.* **1995**, *117*, 546; e) M. W. Mutz, M. A. Case, J. F. Wishart, M. R. Ghadiri, G. L. McLendon, *J. Am. Chem. Soc.* **1999**, *121*, 858.

[5] a) I. Hamachi, S. Tanaka, S. Shinkai, *J. Am. Chem. Soc.* **1993**, *115*, 10458; b) I. Hamachi, S. Tanaka, S.Tsukiji, S. Shinkai, S. Oishi, *Inorg. Chem.* **1998**, *37*, 4380; c) I. Hamachi, S. Tsukiji, S. Tanaka, S. Shinkai, *Chem. Lett.* **1996**, 751; d) I. Hamachi, S. Tsukiji, S. Shinkai, S. Oishi, *J. Am. Chem. Soc.* **1999**, *121*, 5500; e) Y.-Z. Hu, S. Tsukiji, S. Shinkai, I. Hamachi, *Chem. Lett.* **1999**, 517; f) E. Zahavy, I. Willner, *J. Am. Chem. Soc.* **1996**, *118*, 12499; g) I. Willner, E. Zahavy, V. Heleg-Shabtai, *J. Am. Chem. Soc*. **1995**, *117*, 542; h) V. Heleg-Shabtai, T. Gabriel, I. Willner, *J. Am. Chem. Soc.* **1999**, *121*, 3220.

[6] a) Y.-Z. Hu, D. van Loyen, O. Schwarz, S. Bossmann, H. Dürr, V. Huch, M. Veith, *J. Am. Chem. Soc.* **1998**, *120*, 5822; b) Y.-Z. Hu, S. Bossmann, D. van Loyen, O. Schwarz, H. Dürr, *Chem. Eur. J.* **1999**, *5*, 1267.

[7] Y.-Z. Hu, S. Tsukiji, S. Shinkai, S. Oishi, I. Hamachi, *J. Am. Chem. Soc.* **2000**, *122*, 241.

[8] I. Hamachi, H. Takashima, S. Tsukiji, S. Shinkai, T. Nagamune, S. Oishi, *Chem. Lett.* **1999**, 551.

[9] a) K. A. Jolliffe, T. O. M. Bell, K. P. Ghiggino, S. J. Langford, M. N. Paddon-Row, *Angew. Chem.* **1998**, *110*, 959; *Angew. Chem. Int. Ed.* **1998**, *37*, 916; b) M. R. Roest, J. W. Verhoeven, W. Schuddeboom, J. M. Warman, J. M. Lawson, M. N. Paddon-Row, *J. Am. Chem. Soc.* **1996**, *118*, 1762; c) K. Kumar, Z. Lin, D. H. Waldeck, M. B. Zimmt, *J. Am. Chem. Soc.* **1996**, *118*, 243; d) J. N. H. Reek, A. E. Rowan, R. de Gelder, P. T. Beurskens, M. J. Crossley, S. de Feyter, F. de Schryver, R. J. M. Nolte, *Angew. Chem.* **1997**, *109*, 396; *Angew. Chem. Int. Ed. Engl.* **1997**, *36*, 361.

[10] a) E. Itagaki, L. P. Hager, *J. Biol. Chem.* **1966**, *241*, 3687; b) F. S. Mathews, P. H. Bethge, E. W. Czerwinsky, *J. Biol. Chem.* **1979**, *254*, 1699; c) F. Lederer, A. Glatigny, P. H. Bethge, H. D. Bellamy, F. S. Mathews, *J. Mol. Biol.* **1981**, *148*, 427; d) K. Hamada, P. H. Bethge, F. S. Mathews, *J. Mol. Biol.* **1995**, *247*, 947.

[11] a) P.-A. Albertsson, S. Sasakawa, H. Walter, *Nature* **1970**, *228*, 1329; b) S. V. Evans, G. D. Brayer, *J. Mol. Biol*. **1990**, *213*, 885.

[12] It was reported that the redox potential of ZnPP does not significantly change by incorporation of ZnPP into Mb or Cyt; a) M. A. Stanford, B. M. Hoffman, *J. Am. Chem. Soc*. **1981**, *103*, 4104; b) H. Zemel, B. M. Hoffman, *J. Am. Chem. Soc*. **1981**, *103*, 1192; c) N. Barboy, J. Feitelson, *Biochemistry* **1987**, *26*, 3240.

[13] a) N. Liang, A. G. Mauk, G. J. Pielak, J. A. Johnson, M. Smith, B. M. Hoffman, *Science* **1988**, *240*, 311; b) J. M. Nocek, B. P. Sishta, J. C. Cameron, A. G. Mauk, B. M. Hoffman, *J. Am. Chem. Soc*. **1997**, *119*, 2146.

[14] H. Elias, M. H. Chou, J. R. Winkler, *J. Am. Chem. Soc*. **1988**, *110*, 429.

[15] a) T. S. Moore, D. Gust, J.-C. M. Mathis, C. Chachaty, R. V. Bensasson, E. J. Land, D. Doizi, P. A. Liddell, W. R. Lehman, G. A. Nemeth, A. L. Moore, *Nature* **1984**, *307*, 630; b) W. A. Lee, M. Grätzel, K. Kalyanasundaram, *Chem. Phys. Lett.* **1984**, *107*, 308.

[16] Since the stepwise ET pathway in **1** in the abscence of the protein matrix, that is $ZnPP\text{-}{*}Ru^{2+}\text{-}BXV^{4+} \rightarrow ZnPP\text{-}Ru^{3+}\text{-}BXV^{3+\bullet} \rightarrow ZnPP^{+}\text{-}Ru^{2+}\text{-}BXV^{3+\bullet}$, was not observed directly in this study, it is not shown in Scheme 3.

[17] P. D. Barker, J. L. Butler, P. de Oliveria, H. Allen, O. Hill, N. I. Hunt, *Inorg. Chim. Acta* **1996**, *252*, 71.

[18] I. Hamachi, S. Tanaka, S. Tsukiji, S. Shinkai, M. Shimizu, T. Nagamune, *Chem. Commun*. **1997**, 1735.

Received: September 24, 1999 [F2056]

  0947-6539/00/0611-1916 $ 17.50+.50/0